On Parameter Selection for Joint Spectral Reconstruction in Y90 SPECT

Se Young Chun, *Member, IEEE,* Hongki Lim, *Student Member, IEEE,*
Jeffrey A. Fessler, *Fellow, IEEE,* and Yuni K. Dewaraja, *Member, IEEE*

Abstract—Model-based image reconstruction for Y90 SPECT is challenging due to energy-dependent forward models including collimator-detector response (CDR) and attenuation correction factor (ACF). Since it is common to model CDR and ACF for a single energy for one energy window, there is a trade-off between the width of an energy window (number of primary counts) and the accuracy of modeling energy-dependent CDR and ACF. We previously proposed a joint spectral reconstruction (JSR) for Y90 SPECT to utilize wide energy window while accurately modeling energy-dependent forward projections for multiple windows and showed promising quantitative performance. However, the scale parameter model in JSR to relate images of different energy windows was not properly considered. In this work, we argue that scale parameters should reflect two probabilities: 1) different emission probabilities for the different windows and 2) detection probabilities in SPECT crystal that are different for the two windows. These arguments lead us to utilize Monte Carlo simulation of a point source instead of primary phantom counts for estimating scale parameters to avoid the effect of energy-dependent attenuations. We performed a SIMIND MC simulation study with a digital phantom similar to the NEMA PET phantom, but with larger hot spheres and a cold sphere in the center. MC simulation was done with 6 energy windows starting from 105keV to 285keV with the width of 30keV for each window using a new emission spectrum with both internal and external bremsstrahlung generated from theory and Penelope simulations. Our proposed JSR with new scale parameters yielded favorable quantitative results for both hot and cold spheres over other methods such as JSR with previous scale parameters, single spectral reconstructions with narrow and wide energy windows. Our proposed method yielded better recovery coefficients than other methods by 0.5-16.2% at the 30 iteration for all hot spheres. These differences were particularly substantial for the smallest hot sphere, 2.3-16.2%. For the cold sphere, JSR proposed yielded 3.0-15.8% lower residual count error than other methods.

I. INTRODUCTION

QUANTITATIVE yttrium-90 (Y90) imaging is important for absorbed dose estimation in internal emitter therapies with Y90 that have yielded promising clinical results. These therapies include radioembolization for treating nonresectable liver tumors [1] and radioimmunotherapy for non-Hodgkin's

lymphoma [2]. Y-90 SPECT based on imaging bremsstrahlung photons associated with the beta decay of Y90 (average energy, 0.94 MeV; maximum energy 2.3 MeV; mean tissue penetration, 2.5 mm; half-life, 64 h [3]) is more widely accessible compared with Y90 PET that is based on very low abundance positrons and requires state-of-the-art TOF PET systems. However, quantitative bremsstrahlung SPECT is challenging because of the continuous energy spectrum. The high fraction of higher energy downscatter / penetration events that contribute to lower energy acquisition windows cannot be compensated by traditional energy window based scatter correction methods such as triple energy window method.

There have been several works on improving quantitative image quality of Y90 bremsstrahlung SPECT. One approach is to model continuous energy spectrum of Y90 bremsstrahlung in the forward projector of iterative reconstructions. Rong *et al.* proposed multienergy range (MER) SPECT reconstruction that incorporated energy-dependent collimator-detector responses (CDRs), attenuation correction factors, and scatter kernels [4]. Monte-Carlo (MC) simulations were used to estimate CDRs and scatter kernels. However, MER used unmatched forward/backward projectors that may cause convergence issues with some iterative algorithms and used a single energy window acquisition. Yue *et al.* later showed that MER yielded comparable results to Y90 PET-CT in terms of estimating total activity in the liver and activity distributions within treated volumes [5]. Elschot *et al.* proposed a method that is similar to MER, but replaces MER's forward projector with a MC simulator for more accurate forward modeling [6]. Even though this work yielded promising results that are comparable to TOF PET imaging, the proposed method still uses unmatched projectors and it is relatively slow for reconstruction.

We also proposed methods to improve the quantitative imaging quality of Y90 bremsstrahlung SPECT such as a joint spectral reconstruction (JSR) method [7], a MC based scatter correction method [8], and a model for tissue-dependent bremsstrahlung production using CT information [9]. In particular, our JSR method uses matched forward-backward projectors with multi-energy data acquisitions unlike MER. In this article, we investigated parameter selections for JSR in Y90 SPECT, especially parameters in the measurement model for the forward projector of iterative reconstruction algorithms.

II. METHOD

A. Single spectral reconstruction (SSR)

Consider that there is a Y90 tracer distribution in the body. There are certain bremsstrahlung photons that are emitted

within any given energy window through beta decays and only some of which are recorded by the detector. Let us define $\mathbf{x}_e$ (in the unit of counts) be emitted "primary" bremsstrahlung photons within the energy range of the eth energy window that are recorded by the detector. Let us define $\mathbf{A}_e$ be a forward model for the eth energy window that maps from the emitted primary photons to the detectors. Let $\mathbf{y}_e$ be a total measured projection for the eth energy window and $\mathbf{s}_e$ be a (known) scatter projection of the eth energy window. Then, the measurement model is

$$\mathbf{y}_e \sim \text{Poisson}(\mathbf{A}_e \mathbf{x}_e + \mathbf{s}_e) \tag{1}$$

where $\text{Poisson}(\cdot)$ is a component-wise, independent Poisson distribution. The forward model $\mathbf{A}_e$ usually contains attenuation correction information and collimator-detector response (CDR) that are all dependent on energy.

Then, the estimate $\hat{\mathbf{x}}_e$ from the measurement $\mathbf{y}_e$ can be obtained by maximizing the likelihood function as follows:

$$\hat{\mathbf{x}}_e = \arg\max_{\mathbf{x}_e} \text{L}_e(\mathbf{x}_e) \tag{2}$$

where $\text{L}_e(\mathbf{x}_e) := \text{L}(\cdot; \mathbf{A}_e, \mathbf{y}_e, \mathbf{s}_e)$ is the sum of Poisson log-likelihood functions with $\mathbf{A}_e$, $\mathbf{y}_e$, and $\mathbf{s}_e$ for the eth energy window. This optimization is usually done by an iterative algorithm such as ordered-subset expectation-maximization (OS-EM) [10] as follows:

$$\hat{\mathbf{x}}_e^{(n,m+1)} = \hat{\mathbf{x}}_e^{(n,m)} + \frac{\hat{\mathbf{x}}_e^{(n,m)}}{\mathbf{A}'_{e,m}\mathbf{1}} \nabla \text{L}_{e,m}(\hat{\mathbf{x}}_e^{(n,m)}) \tag{3}$$

where $\text{L}_{e,m}(\hat{\mathbf{x}}_e^{(n,m)}) := \text{L}(\hat{\mathbf{x}}_e^{(n,m)}; \mathbf{A}_{e,m}, \mathbf{y}_{e,m}, \mathbf{s}_{e,m})$ is the log-likelihood function of the eth energy window and the mth subset, n is an iteration number, $\mathbf{A}_{e,m}$, $\mathbf{y}_{e,m}$, and $\mathbf{s}_{e,m}$ are forward model, total projection, and scatter projection for the eth energy window and the mth subset, respectively.

With a narrow energy window (*e.g.*, 105-135 keV), accurate modeling for $\mathbf{A}_e$ is possible by using CDR and attenuation correction information at the mean energy of that window. However, there may not be enough counts in a narrow energy window for good reconstruction quality. We denote this narrow energy window case by SSR-N, single spectral reconstruction with narrow window. With a wide energy window (*e.g.*, 105-285 keV), enough counts will be available for low noise reconstruction, but at the price of degrading the model accuracy for $\mathbf{A}_e$ with mean energy based CDR and attenuation correction. We denote this wide energy window case by SSR-W, SSR with wide energy window.

B. Emitted photon model in multiple energy windows

The authors proposed joint spectral reconstruction (JSR) for Y-90 SPECT by modeling emitted bremsstrahlung photons in multiple energy windows that are associated with underlying Y90 activity distributions using simple scale parameters [7]. Consider a total emitted bremsstrahlung photons $\mathbf{x}$. Then, for the emitted photons $\mathbf{x}_e$ in the eth energy window, the following relationship should be true:

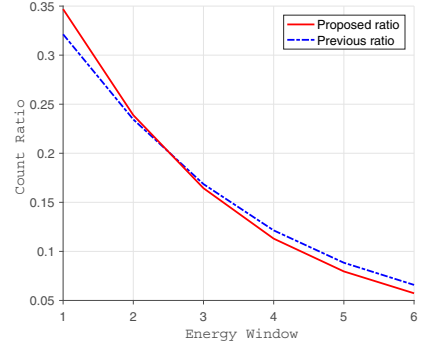$$\mathbf{x} = \sum_e \mathbf{x}_e. \tag{4}$$

Fig. 1. Scale parameters estimated from phantom sinogram data (Previous ratio) and from point source simulation data (Proposed ratio). Different parameters were estimated due to energy-dependent attenuations.

In [7], we modeled the emitted bremsstrahlung photons $\mathbf{x}_e$ as proportional to the total emitted photons $\mathbf{x}$:

$$\mathbf{x}_e = \tau_e \mathbf{x} \tag{5}$$

where τ_e is a scale parameter to describe the ratio of emitted photons in the eth energy window to total emitted photons in all energy ranges. These τ_e were able to be inferred using primary counts $(\mathbf{y}_e - \mathbf{s}_e)$ in all energy windows [7]. We denote this method by "JSR previous".

In this work, we argue that the scale parameters τ_e should reflect two probabilities:

1) emission probabilities that are different for the different windows (that go down with energy)
2) detection probabilities in SPECT crystal that are different for the two windows (that also go down with energy).

Since the primary counts $(\mathbf{y}_e - \mathbf{s}_e)$ [7] may include factors other than these two probabilities due to energy dependent attenuation, we propose to measure these scale parameters using a quick MC simulation of a point source at 10 cm distance between the detector and the source. We denote this method by "JSR proposed". Fig. 1 shows estimated scale parameters in 6 energy windows using phantom data (Previous ratio) and using point source MC simulation (Proposed ratio). As expected, our proposed method yielded higher scale parameter than previous method near low energy due to high attenuation on low energy windows. Further analyses on the effect of this proposed scale parameters for JSR will be in the next section.

C. Joint spectral reconstruction (JSR)

In [7], JSR was derived based on the following probabilistic model:

$$\begin{bmatrix} \vdots \\ \mathbf{y}_e \\ \vdots \end{bmatrix} \sim \text{Poisson}\left(\begin{bmatrix} \vdots \\ \mathbf{A}_e \tau_e \\ \vdots \end{bmatrix} \mathbf{x} + \begin{bmatrix} \vdots \\ \mathbf{s}_e \\ \vdots \end{bmatrix} \right). \tag{6}$$

Then, the OS-EM for JSR can be derived as follows:

$$\hat{\mathbf{x}}^{(n,m+1)} = \hat{\mathbf{x}}^{(n,m)} + \frac{\hat{\mathbf{x}}^{(n,m)}}{\sum_{e'} \tau_{e'} \mathbf{A}'_{e',m}\mathbf{1}} \sum_e \nabla \tilde{\text{L}}_{e,m}(\hat{\mathbf{x}}^{(n,m)}) \tag{7}$$

where $\tilde{\text{L}}_{e,m}(\hat{\mathbf{x}}^{(n,m)}) := \text{L}(\hat{\mathbf{x}}^{(n,m)}; \mathbf{A}_{e,m}\tau_e, \mathbf{y}_{e,m}, \mathbf{s}_{e,m})$.

One interpretation of (7) is that the next update for reconstructed image is

$$\sum_{e=1}^{E}\left\{\hat{\mathbf{x}}_e^{(n,m)} + \frac{\hat{\mathbf{x}}^{(n,m)}}{\sum_{e'}\tau_{e'}\mathbf{A}'_{e',m}\mathbf{1}}\nabla \mathrm{L}_{e,m}(\hat{\mathbf{x}}_e^{(n,m)})\right\} \quad (8)$$

where $\hat{\mathbf{x}}_e^{(n,m)} = \tau_e\hat{\mathbf{x}}^{(n,m)}$. However, we observed that this algorithm often yielded slow convergence compared to SSR methods. We propose to relax (8) as follows:

$$\sum_{e=1}^{E}\left\{\hat{\mathbf{x}}_e^{(n,m)} + \frac{\hat{\mathbf{x}}^{(n,m)}}{\sum_{e'}\tau_{e'}\mathbf{A}'_{e',m}\mathbf{1}}E\tau_e\nabla \mathrm{L}_{e,m}(\hat{\mathbf{x}}_e^{(n,m)})\right\} \quad (9)$$

where E is the number of energy windows. We over-relaxed the algorithm associated with low energy windows considering that they have high primary count ratios and accurate CDR modeling. We under-relaxed the algorithm associated with high energy windows considering the difficulties of modeling accurate CDR and low primary counts with very high scatter counts. Thus, the final relaxed OS-EM algorithm is

$$\hat{\mathbf{x}}^{(n,m+1)} = \hat{\mathbf{x}}^{(n,m)} + \frac{\hat{\mathbf{x}}^{(n,m)}}{\sum_{e'}\tau_{e'}\mathbf{A}'_{e',m}\mathbf{1}} \times \quad (10)$$
$$\sum_e E\tau_e\nabla\tilde{\mathrm{L}}_{e,m}(\hat{\mathbf{x}}^{(n,m)}).$$

The implementation of this relaxed OS-EM can be done by modifying OS-EM for SSR: summing the gradients of cost functions for all energy windows and then dividing it by the sum of sensitivity images. In our previous work, we used the estimated scale parameters from the phantom data $(\mathbf{y}_e - \mathbf{s}_e)$ for τ_e. In here, we propose to estimate them from MC point source simulation.

III. SIMULATION RESULTS

A. Simulation setup

We performed a MC simulation study using SIMIND [11] with a digital phantom ($128\times128\times128$ voxels with $4.8\mathrm{mm}\times4.8\mathrm{mm}\times4.8\mathrm{mm}$ per voxel) similar to the NEMA PET phantom [12], but with larger hot spheres (about 2, 4, 8, 17, 27, 100 mL) more appropriate for SPECT and a cold sphere in the center. SIMIND MC simulation was done with the acquisition energy windows of 105-135, 135-165, 165-195, 195-225, 225-255, 255-285 keV (6 windows). Note that our SIMIND MC simulation used a new bremsstrahlung emission spectrum with both internal and external bremsstrahlung generated from theory (for IB) and Penelope simulations (for EB) [13]. We selected these 6 windows based on the fact that the primary to scatter ratio drops off rapidly with energy and to avoid x-ray and high order scatter at low energies. We also simulated a point source emission for the same measurement energy windows to determine scale parameters for JSR.

Using MC simulated projection data, a Poisson realization was obtained assuming 100 million counts for 105-195 keV energy range. Four reconstruction methods were performed: SSR-N (105-135 keV), SSR-W (105-285 keV), JSR previous (105-285 keV), and JSR proposed (105-285 keV). The true scatter from MC was used, but it can be estimated by MC based scatter correction.

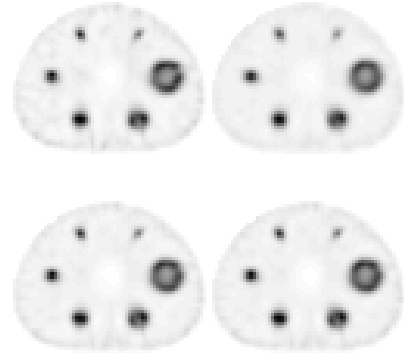**Reconstructed images at 40th iteration (4 subsets)**

Fig. 2. Reconstructed images at the 40 iteration using SSR-N (top left), SSR-W (top right), JSR proposed (bottom left), JSR previous (bottom right).

Assuming that estimated emitted photon count is proportional to Y90 activity, we first calibrate to yield an estimated Y90 activity using the total counts in the field of view. We used the following metrics to assess the quantitative accuracy of all reconstruction methods: For hot spheres,

$$\mathrm{RC}_{\mathrm{ROI}} = \frac{\text{mean estimated activity in ROI}}{\text{mean true activity in ROI}}$$

where RC, ROI stand for recovery coefficient, region of interest, respectively. For cold sphere with 0 activity,

$$\mathrm{RCE}_{\mathrm{ROI}} = \frac{\text{mean estimated activity in ROI}}{\text{mean estimated activity in BG}}$$

where RCE, BG stand for residual count error, background, respectively. Ideally, RC should be 1 and RCE should be 0.

B. Quantitative and qualitative results

Fig. 2 shows four reconstructed images. SSR-N seems to yield noisier reconstructed image than other methods due to the lack of counts and SSR-W seems to yield blurrier image than other methods due to inaccurate forward model. However, these differences are not very substantial visually.

Fig. 3 shows that our "JSR proposed" yielded the lowest normalized activity (RCE) over iteration among all other methods for a cold sphere. In RCE, it seems important to model a forward projector accurately to yield good quantitative results
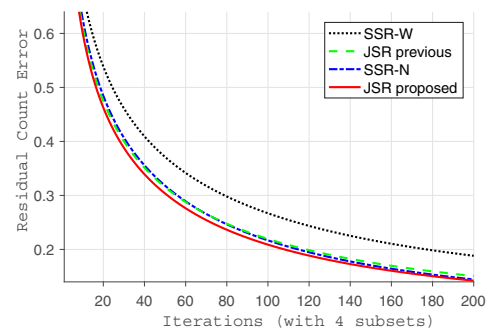

Fig. 3. RCE over iteration for SSR-N, SSR-W, JSR previous, JSR proposed. JSR proposed yielded the lowest RCE over iteration.
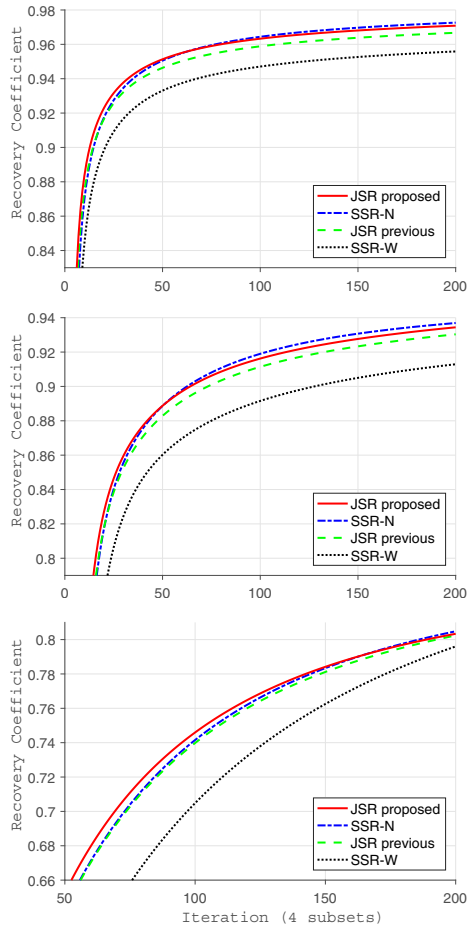
Fig. 4. RCs over iterations for the hot spheres of 98.5mL, 15.6mL, and 1.7mL. JSR proposed yielded better RCs than JSR previous and SSR-W and RCs close to those of SSR-N for hot spheres.
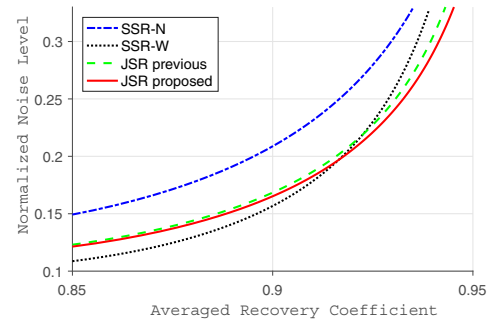

Fig. 5. Weighted average of RCs vs. normalized noise level over iterations. At high RC values, JSR proposed achieved the lowest normalized noise level among all methods including JSR previous.

quantitative results for RC in hot spheres, RCE in cold sphere, and RC-noise trade-off.

since SSR-W yielded substantially worse RCE than other methods. Note also that our JSR proposed yielded lower RCE than JSR previous, which illustrates that our proposed scale parameter estimation works better than previous estimation method.

JSR proposed yielded better RCs than JSR previous and SSR-W and RCs close to those of SSR-N for hot spheres as illustrated in Fig. 4. In particular, it achieved the best RC for all hot spheres at early iterations by small margins (*e.g.*, 0.31-7.91% at the 30 iteration). These differences were particularly substantial for the smallest sphere (1.7 mL), 1.29-7.91% at the 30 iteration.

Lastly, Fig. 5 shows the curves of normalized noise level in BG vs. weighted average of RCs for all hot spheres with the weights that are proportional to sphere volumes. Normalized noise level is defined to be the standard deviation in BG over the mean activity in BG. At high RC values, JSR proposed achieved the lowest normalized noise level among all methods including JSR previous.

IV. CONCLUSION

We proposed a method to estimate scale parameters for JSR using a point source MC simulation. With our relaxed OS-EM, our proposed method (JSR proposed) yielded favorable

REFERENCES

[1] A. Kennedy, "Radioembolization of hepatic tumors," *Journal of gastrointestinal oncology*, vol. 5, no. 3, pp. 178–189, Jun. 2014.

[2] S. J. Goldsmith, "Radioimmunotherapy of Lymphoma: Bexxar and Zevalin," *Seminars in Nuclear Medicine*, vol. 40, no. 2, pp. 122–135, Mar. 2010.

[3] M. D'Arienzo, "Emission of $\beta+$ Particles Via Internal Pair Production in the 0+ − 0+ Transition of 90Zr: Historical Background and Current Applications in Nuclear Medicine Imaging," *Atoms*, vol. 1, no. 1, pp. 2–12, Mar. 2013.

[4] X. Rong, Y. Du, M. Ljungberg, E. Rault, S. Vandenberghe, and E. C. Frey, "Development and evaluation of an improved quantitative 90Y bremsstrahlung SPECT method," *Medical Physics*, vol. 39, no. 5, pp. 2346–14, 2012.

[5] J. Yue, T. Mauxion, D. K. Reyes, M. A. Lodge, R. F. Hobbs, X. Rong, Y. Dong, J. M. Herman, R. L. Wahl, J.-F. H. Geschwind, and E. C. Frey, "Comparison of quantitative Y-90 SPECT and non-time-of-flight PET imaging in post-therapy radioembolization of liver cancer," *Medical Physics*, vol. 43, no. 10, pp. 5779–5790, Sep. 2016.

[6] M. Elschot, M. G. E. H. Lam, M. A. A. J. van den Bosch, M. A. Viergever, and H. W. A. M. de Jong, "Quantitative Monte Carlo-Based 90Y SPECT Reconstruction," *Journal of Nuclear Medicine*, vol. 54, no. 9, pp. 1557–1563, Sep. 2013.

[7] M. P. Nguyen, H. Kim, S. Y. Chun, J. A. Fessler, and Y. K. Dewaraja, "Joint spectral image reconstruction for Y-90 SPECT with multi-window acquisition," in *IEEE Nuclear Science Symposium and Medical Imaging Conference*, 2015, pp. 1–4.

[8] Y. K. Dewaraja, S. Y. Chun, R. N. Srinivasa, R. K. Kaza, K. C. Cuneo, B. S. Majdalany, P. M. Novelli, M. Ljungberg, and J. A. Fessler, "Improved quantitative 90Y bremsstrahlung SPECT/CT reconstruction with Monte Carlo scatter modeling," *Medical Physics*, vol. 5, pp. 178–13, Oct. 2017.

[9] H. Lim, J. A. Fessler, S. J. Wilderman, A. F. Brooks, and Y. K. Dewaraja, "Y-90 SPECT ML image reconstruction with a new model for tissue-dependent bremsstrahlung production using CT information: a proof-of-concept study," *Physics in Medicine & Biology*, vol. 63, no. 11, pp. 115 001–115 009, Nov. 2018.

[10] H. M. Hudson and R. S. Larkin, "Accelerated image reconstruction using ordered subsets of projection data," *IEEE Transactions on Medical Imaging*, vol. 13, no. 4, pp. 601–609, 1994.

[11] M. Ljungberg, "The SIMIND Monte Carlo Program," in *Monte Carlo Calculations in Nuclear Medicine*, M. Ljungberg, S.-E. Strand, and M. A. King, Eds., Boca Raton, 2012, pp. 111–128.

[12] M. E. Daube-Witherspoon, J. S. Karp, M. E. Casey, F. P. DiFilippo, H. Hines, G. Muehllehner, V. Simcic, C. W. Stearns, L.-E. Adam, S. Kohlmyer, and V. Sossi, "PET performance measurements using the NEMA NU 2-2001 standard," *Journal of Nuclear Medicine*, vol. 43, no. 10, pp. 1398–1409, Oct. 2002.

[13] Y. Dewaraja, R. Fleming, P. Simpson, S. Walrand, M. Ljungberg, and S. Wilderman, "Impact of internal bremsstrahlung on Y-90 SPECT Imaging," *Journal of Nuclear Medicine*, vol. 59, no. supplement 1, p. 577, May 2018.